



## OPEN

# Isogambogenic acid induces apoptosis-independent autophagic cell death in human non-small-cell lung carcinoma cells

SUBJECT AREAS:  
NON-SMALL-CELL LUNG  
CANCER  
MACROAUTOPHAGY

Received  
27 February 2014

Accepted  
4 December 2014

Published  
9 January 2015

Correspondence and requests for materials should be addressed to L.J.C. (chenlijuan125@163.com) or W.M.L. (weimi003@yahoo.com)

\* These authors contributed equally to this work.

Jianhong Yang<sup>1\*</sup>, Yongzhao Zhou<sup>2\*</sup>, Xia Cheng<sup>1\*</sup>, Yi Fan<sup>1</sup>, Shichao He<sup>1</sup>, Shucui Li<sup>1</sup>, Haoyu Ye<sup>1</sup>, Caifeng Xie<sup>1</sup>, Wenshuang Wu<sup>1</sup>, Chunyan Li<sup>1</sup>, Heying Pei<sup>1</sup>, Luyuan Li<sup>3</sup>, Zhe Wei<sup>1</sup>, Aihua Peng<sup>1</sup>, Yuquan Wei<sup>1</sup>, Weimin Li<sup>2</sup> & Lijuan Chen<sup>1</sup>

<sup>1</sup>State Key Laboratory of Biotherapy/Collaborative Innovation Center of Biotherapy and Cancer Center, West China Hospital of Sichuan University; Chengdu, China, <sup>2</sup>Department of Respiratory Medicine, West China Hospital of Sichuan University, Chengdu, China, <sup>3</sup>State Key Laboratory of Medicinal Chemical Biology and Nankai University College of Pharmacy, Tianjin, China.

**To overcome drug resistance caused by apoptosis deficiency in patients with non-small cell lung carcinoma (NSCLC), there is a need to identify other means of triggering apoptosis-independent cancer cell death. We are the first to report that isogambogenic acid (iso-GNA) can induce apoptosis-independent autophagic cell death in human NSCLC cells. Several features of the iso-GNA-treated NSCLC cells indicated that iso-GNA induced autophagic cell death. First, there was no evidence of apoptosis or cleaved caspase 3 accumulation and activation. Second, iso-GNA treatment induced the formation of autophagic vacuoles, increased LC3 conversion, caused the appearance of autophagosomes and increased the expression of autophagy-related proteins. These findings provide evidence that iso-GNA induces autophagy in NSCLC cells. Third, iso-GNA-induced cell death was inhibited by autophagic inhibitors or by selective ablation of *Atg7* and *Beclin 1* genes. Furthermore, the mTOR inhibitor rapamycin increased iso-GNA-induced cell death by enhancing autophagy. Finally, a xenograft model provided additional evidence that iso-GNA exhibited anticancer effect through inducing autophagy-dependent cell death in NSCLC cells. Taken together, our results demonstrated that iso-GNA exhibited an anticancer effect by inducing autophagy-dependent cell death in NSCLC cells, which may be an effective chemotherapeutic agent that can be used against NSCLC in a clinical setting.**

Lung cancer causes approximately 1.4 million deaths annually, as reported in 2008<sup>1</sup>. Despite the fact that many therapeutic approaches are available, deaths due to lung cancer have continued to increase in recent years. Resistance to chemotherapy is one of the main obstacles for the treatment of lung cancers.

Platinum-based drugs are widely used to treat patients with NSCLC in clinical. However, drug-resistance commonly develops in these patients. For instance, approximately 70% of NSCLC patients with advanced unresectable or widespread incurable metastasis are candidates for neoadjuvant or palliative chemotherapy. However, approximately two-thirds of these patients do not benefit from conventional chemotherapy<sup>2</sup>. Subsequent research revealed that conventional chemotherapy is unable to induce apoptosis-dependent cell death in 60% of these NSCLC patients. In these patients, apoptosis deficiency is a very important mechanism for platinum-based drug-resistance in NSCLC<sup>2-3</sup>. Therefore, it is of great importance to develop new compounds that can induce apoptosis-independent cell death with a lower frequency of resistance.

Chemotherapeutics often exert anti-cancer effects through induction of apoptosis-dependent cancer cell death. Autophagic cell death, a new cell death pathway, has become another mechanism for cancer cell death induced by chemotherapeutics in recent years<sup>4-8</sup>. Although autophagy has pro-survival functions in response to cancer therapeutics, which could reduce drug efficacy<sup>9-13</sup>, studies of autophagy as an important mechanism for cancer cell death have also been reported in recent years<sup>14,15</sup>, and various treatments have been shown to induce autophagic cell death<sup>16,17</sup>. Despite the fact that the mechanisms of autophagy in cancer is not well defined, cancer treatment aimed at inducing autophagic cell death are becoming another choice for cancer treatment.



The main physiological function of autophagy is to degrade cytoplasmic macromolecules and endogenous substrates to maintain cell homeostasis. Autophagic vacuoles in the cytoplasm and intact nucleus in the late stage of cell death are typical features of autophagic cell death. In addition, during autophagy, some autophagy-related proteins are also activated. For example, Atg6/Beclin1 is activated to form autophagosome during the initiation stage of autophagy<sup>18</sup>, and the Atg12-Atg5 complex and Atg8/LC3 played an important role in mediating the autophagosome expansion<sup>19</sup>. Autophagy is a strictly regulated cellular pathway that can be activated by various stimuli through different signaling pathways. These stimuli include nutrient deprivation, an excess of reactive oxygen species and DNA damage<sup>20</sup>. Among the involved signaling pathways, the classic Akt/mTOR pathway acted as a negative regulator of autophagy<sup>21</sup>.

Gambogic acid (GA), a natural product from *Garcinia hanburyi*, showed anticancer activity by inducing apoptosis-dependent cancer cell death<sup>22</sup>. GA has been approved by the State Food and Drug Administration (SFDA) of China for phase II clinical trials to treat lymphatic sarcoma, breast cancer and carcinoma cutaneum<sup>23</sup>. However, isogambogenic acid (iso-GNA), another main component of *Garcinia hanburyi*, had not been investigated for its biological function until we first reported that it exhibits anti-cancer activities by inhibiting tumor angiogenesis<sup>23</sup>. In further studies of the anti-tumor mechanism of iso-GNA, we found that it failed to induce apoptosis even at high concentrations (in contrast with GA). Surprisingly, iso-GNA could induce autophagic cancer cell death in NSCLC cells. Our study elucidated the mechanism of the anticancer activity of iso-GNA and indicated that iso-GNA may be an effective chemotherapeutic agent against NSCLC in a clinical setting.

## Results

**Anti-Cancer Activities of Iso-GNA.** The viability of human cancer cells treated with iso-GNA (Fig. 1A) was examined by MTT assay *in vitro*. Iso-GNA showed a strong cytotoxic effect (Fig. 1B). The IC<sub>50</sub> of iso-GNA was approximately 5–15  $\mu$ M for several tumor cell lines. Additionally, iso-GNA dose and time-dependently inhibited cell viability in both A549 and H460 cell lines (Fig. 1C, 1D). Then we established a NSCLC (A549) xenograft mouse model to investigate the anti-cancer ability of iso-GNA *in vivo*. The results showed that intravenous administration (tail vein, 20 mg/kg) of iso-GNA caused a significant reduction of tumor volume and weight (Fig. 1E and 1F). The inhibitory rate for tumors in the iso-GNA-treated group was 76% compared with the untreated group. So, both the *in vitro* and *in vivo* study showed that iso-GNA possessed good anti-cancer activities.

**Iso-GNA Induces Cancer Cell Death Via An Apoptosis-Independent Pathway.** To examine whether iso-GNA affected cell cycle and induced apoptosis in tumor cell lines, we performed flow cytometry analysis. Iso-GNA induced a slight G0/G1 phase accumulation but did not appear to induce apoptosis in A549 cells. By contrast, cisplatin (positive control) induced both an obvious G0/G1 phase accumulation and apoptosis (Fig. 2A).

To further investigate whether iso-GNA could induce apoptosis in NSCLC cells, we examined the apoptotic effect of iso-GNA in A549 and H460 cells using a PI/Annexin V flow cytometric assay (Fig. 2B, S1A). We found that obvious apoptosis was caused by cisplatin (positive control) in a concentration-dependent manner. By contrast, iso-GNA did not induce obvious apoptosis at the indicated concentrations, which could cause major cell death, suggesting that iso-

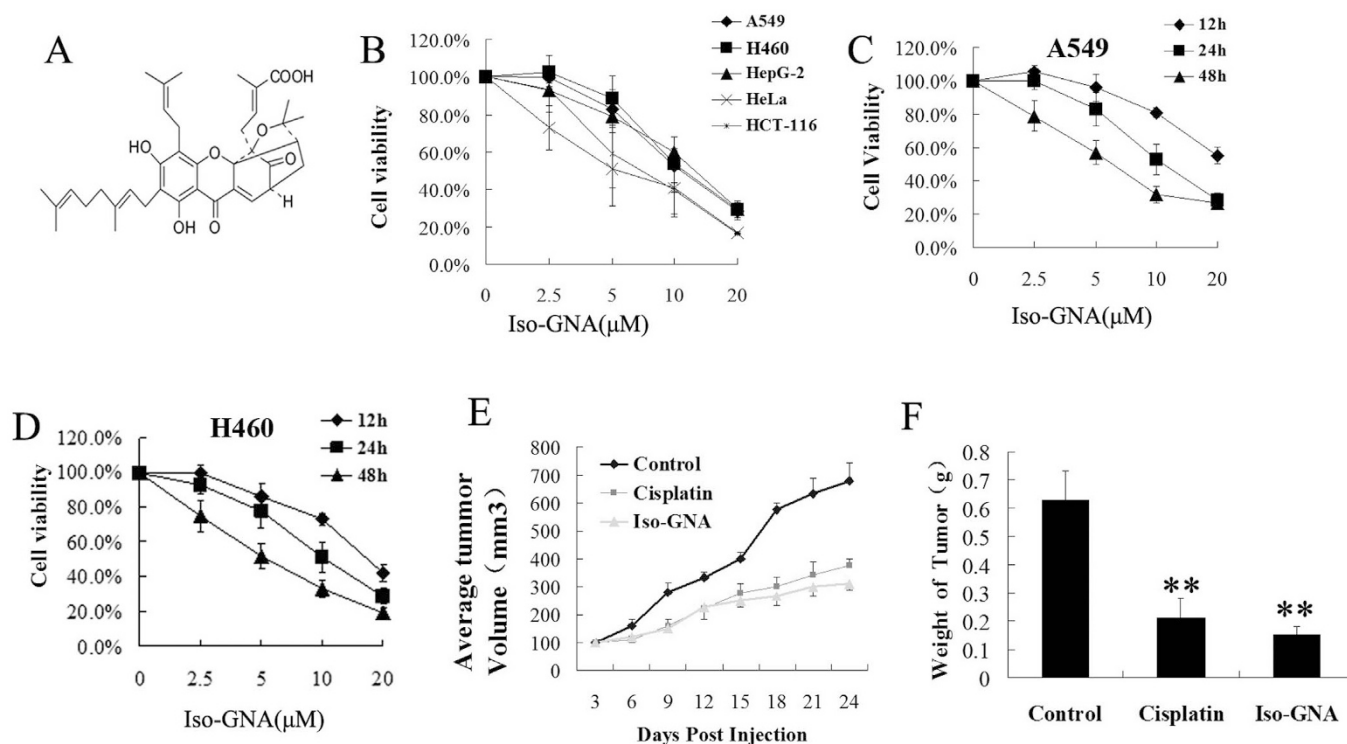


**Figure 1 | Anti-Cancer Activities of Iso-GNA.** (A) Structure of iso-GNA. (B) A549, H460, HepG2, HeLa and HCT-116 cell were incubated with 0, 2.5, 5, 10  $\mu$ M of iso-GNA for 24 h. MTT assay was employed to detect cell viability. (C) and (D) Human NSCLC A549 (C) or H460 (D) cells were incubated with 0, 2.5, 5, 10  $\mu$ M of iso-GNA for various times. MTT assay was employed to detect cell viability. (E) and (F) Mice were injected with or without iso-GNA (20 mg/kg/2 days) after solid tumours grew to 70 mm<sup>3</sup>, the positive control group was treated with cisplatin (4 mg/kg/two times per week). The solid tumor growth was inhibited by iso-GNA as measured by relative tumour volume (E) and weight (F). \*\* $p < 0.01$ , in comparison with the untreated group.

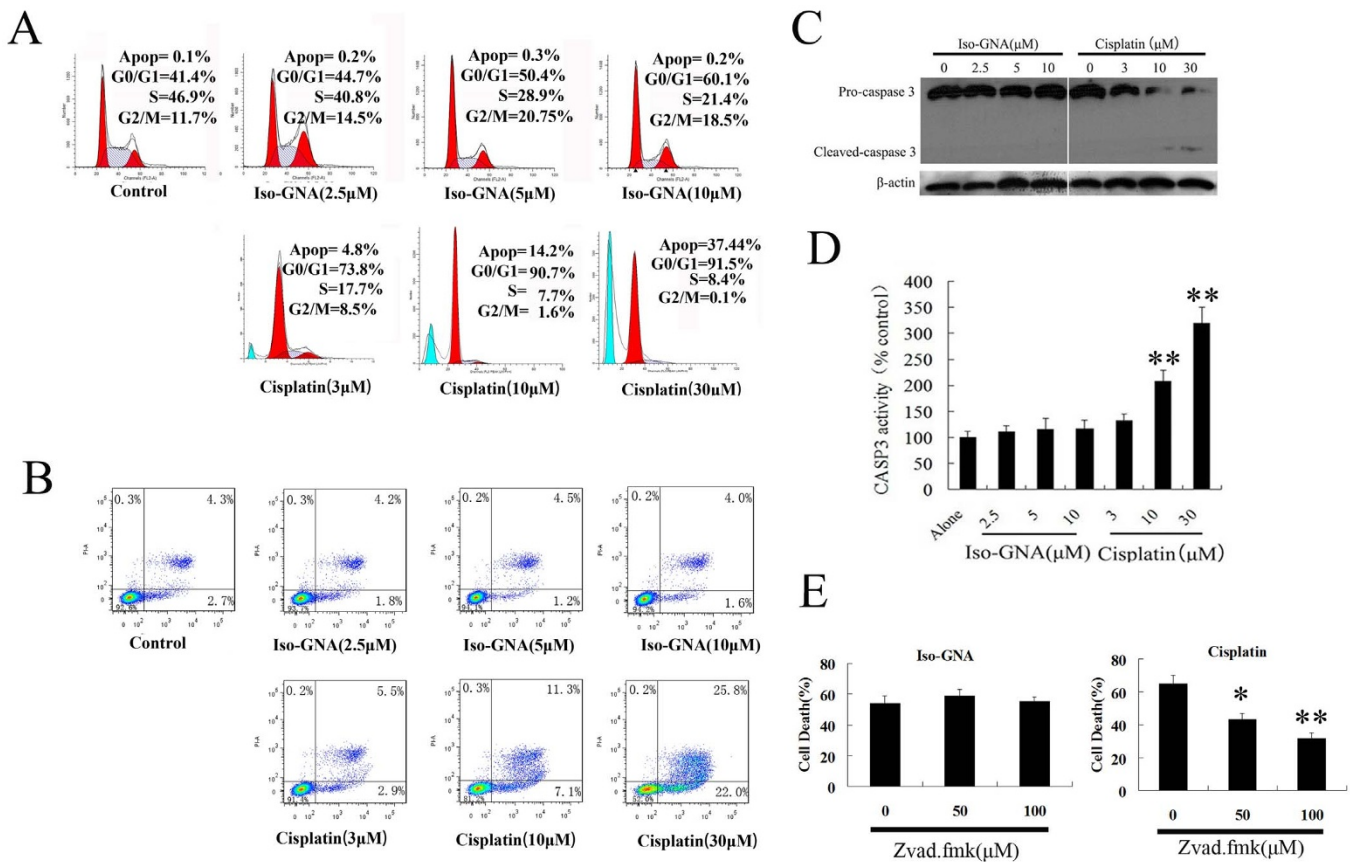


**Figure 2 | Iso-GNA Induced Human NSCLC A549 Cell Death Was Apoptosis-Independent.** (A) and (B) A549 ( $5 \times 10^5$  cells per well) cells were seeded on 6-well plates for 24 h and then incubated with indicated concentrations of iso-GNA or cisplatin for 24 h. then (A) cells were stained with PI before cell cycle analysis by flow cytometry. (B) Cells were stained with Annexin V-FITC/PI before cell apoptosis analysis by flow cytometry. (C) Expression of caspase3 in A549 cells. Different concentrations of iso-GNA or cisplatin were incubated with A549 cells for 24 h, then western blot was performed to analyze caspase3 expression. (D) Caspase3 activity in A549 cells. Different concentrations of iso-GNA or cisplatin were incubated with A549 cells for 24 h, and then subjected to analyze Caspase3 activity. (E) Caspase-independent cell death caused by iso-GNA. Different concentrations of zVAD.fmk was added to A549 cells for 6 h before the treatment of 10  $\mu$ M iso-GNA or 30  $\mu$ M cisplatin for 36 h, then cells were stained with trypan blue to analyze death ratio. Data of three independent tests were shown as means  $\pm$  s.d. \* $p < 0.5$ ; \*\* $p < 0.01$ , in comparison with the untreated group. The whole images of western blots are given in Supplementary Figure S6.

GNA failed to induce apoptosis. In accordance with the *in vitro* observations, immunohistochemical analysis by TUNEL of tumor sections from A549-bearing nude mice treated with iso-GNA showed very little apoptosis (Fig. 1B). However, a number of TUNEL-positive cells appeared in cisplatin-treated tumor sections. Western blot further revealed that cisplatin-treated A549 and H460 cells accumulated cleaved caspase 3. By contrast, no cleaved caspase 3 accumulation was detected in A549 and H460 cells treated with iso-GNA (Fig. 2C, S1C). Then caspase 3 enzyme activity assay was used to detect whether caspase 3 was activated in A549 and H460 cells treated with iso-GNA. As shown in Fig. 2D and S1D, iso-GNA did not cause an obvious increase in caspase 3 activity, whereas cisplatin caused an increase of caspase 3 activity as concentrations increased. Furthermore, different concentrations of zVAD.fmk, an apoptosis inhibitor, were exposed to A549 and H460 cells for 6 h, and then 10  $\mu$ M iso-GNA or 30  $\mu$ M cisplatin were incubated with the cells for 36 h. Subsequently, cells were collected and stained with trypan blue to test the cell death ratio. We found that cell death caused by cisplatin, but not iso-GNA, was obviously blocked by zVAD.fmk (Fig. 2E and S1E). All these results indicated that cell death induced by iso-GNA in A549 and H460 cells were apoptosis-independent.

**Iso-GNA Induces Autophagy in A549 and H460 Cells.** Because the cytotoxic effect of iso-GNA was not due to caspase-dependent cell

death, we examined whether the cytotoxic effect of iso-GNA was caused by autophagy. The expression level of the general autophagosomal marker LC3-II was tested firstly in our study<sup>24</sup>. As shown in Figure 3A and S2A, treatment with iso-GNA for 24 h in A549 and H460 cells could increase the expression level of LC3-II, and the increased expression level of LC3-II could be inhibited by 3-MA (3-methyladenine), a specific autophagy inhibitor. In accordance with the *in vitro* study, *in vivo* NSCLC xenograft mouse model provided additional evidence that accumulation of LC3 was increased in response to iso-GNA treatment (Fig. S2B).

In addition to LC3, SQSTM1/p62 is another frequently-used autophagy marker. P62 protein linked LC3 and the ubiquitinated proteins during autophagy. As polyubiquitinated substrates are transferred into the intact autophagosome to degrade in autolysosomes, p62 is also degraded with p62-bound ubiquitinated substrate. Therefore, p62 is identified as a negative marker of autophagic degradation<sup>25</sup>, and the clearance of p62 may be a positive indicator of autophagy. In our study, we observed p62 clearance in iso-GNA-treated A549 cells (Fig. 3B).

Then, we used the RFP-LC3 (red fluorescent protein-fused LC3) to detect autophagy. A549 cells stably expressing RFP-LC3 were selected by G418 (Fig. S2C). As indicated in Figure 3C, iso-GNA induced membrane aggregation of RFP-LC3 fluorescent spots, while the untreated cells showed only diffuse RFP-LC3 fluorescent dots.



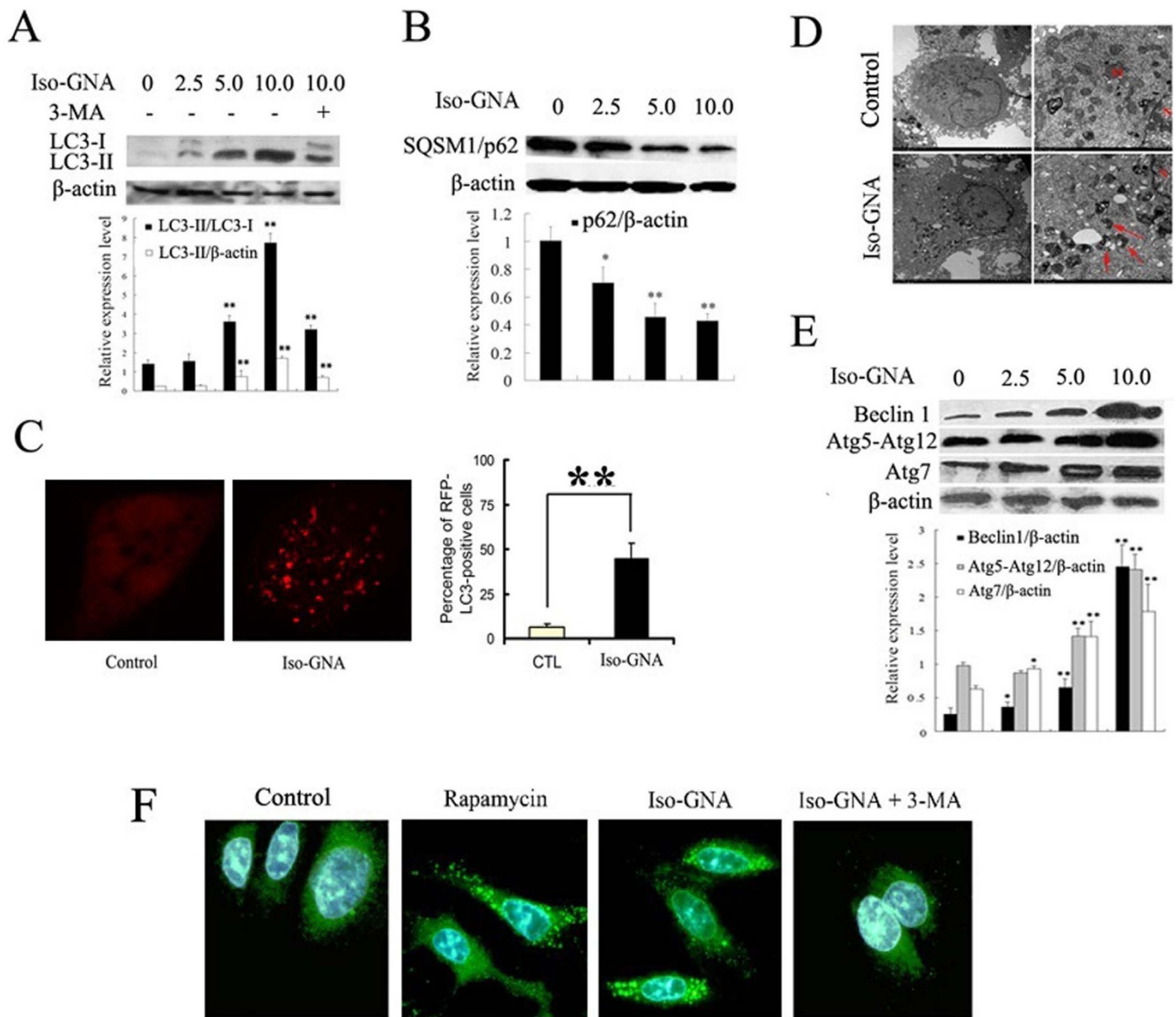


**Figure 3 | Evident Autophagy Was Observed in Iso-GNA Treated 549 cells.** (A) LC3 expression in A549 cells. Different concentrations of iso-GNA were incubated with A549 cells for 24 h. and 3-MA (2 mM) was treated as an autophagy inhibitor. (B) SQSTM1(p62) expression in A549 cells. Different concentrations of iso-GNA were incubated with A549 cells for 24 h. (C) 10 μM iso-GNA were treated with A549 cells (expression RFP-LC3) for 24 h. RFP-LC3 dots was observed by Leica aser-scanning spectrum confocal system. (D) 10 μM iso-GNA were treated with A549 cells for 24 h, then cells were subjected to transmission electron microscopy to observe double-membraned vacuolation (arrows) (E) Various concentrations of iso-GNA were treated with A549 cells for 24 h. then Beclin 1, Atg7 and Atg12-Atg5 complex expression level were detected by western blot. (F) A549 cells treated with 2 μM rapamycin, 10 μM iso-GNA with or without 4 mM 3-MA for 24 h. Then LC3 immunofluorescence image in A549 cells were detected by a fluorescence microscope. Data of three independent tests were shown as means ± s.d. \**p* < 0.5; \*\**p* < 0.01, in comparison with the untreated group. The whole images of western blots are given in Supplementary Figure S7.

The LC3 recruitment effect was further confirmed by an immunofluorescence assay. As exhibited in Fig 3F, the vehicle-treated cells showed weak, punctate LC3 expression. By contrast, cells with iso-GNA or rapamycin (positive control) showed green, punctate LC3 throughout the cytoplasm. This effect could be inhibited by the addition of 3-MA, demonstrating that LC3 accumulated in iso-GNA-induced autophagy.

As the formation of autophagic vacuoles with double-membrane in the cytoplasm is a common feature of autophagy<sup>26</sup>, which can be observed using transmission electron microscopy. Therefore, we examined the subcellular structures of autophagic vesicles in iso-GNA-treated A549 cells. The results show that multiple membrane-covered vesicles appeared in the cytoplasm of iso-GNA-treated A549

cells (Fig. 3D), suggesting that iso-GNA caused the formation of autophagic vacuoles.

Once autophagy is induced, the expression level of various autophagy-related proteins connected with the initiation and elongation of the autophagosome will be greatly upregulated<sup>27</sup>. Vesicle nucleation in the initiating stage of autophagy is accomplished through the activation of a complex composed of Beclin1/Atg6 and other proteins. The subsequent vesicle elongation stage is achieved as a result of two ubiquitin-like conjugation systems<sup>28</sup>. One of them, Atg7, is an E1 ubiquitin conjugase-like enzyme that facilitates conjugation of LC3 (ATG8) proteins to PE and acts as an E1 enzyme to form ATG5-ATG12 complex and then from autophagic vacuoles<sup>28</sup>. We used western blot to investigate whether the expression levels of the

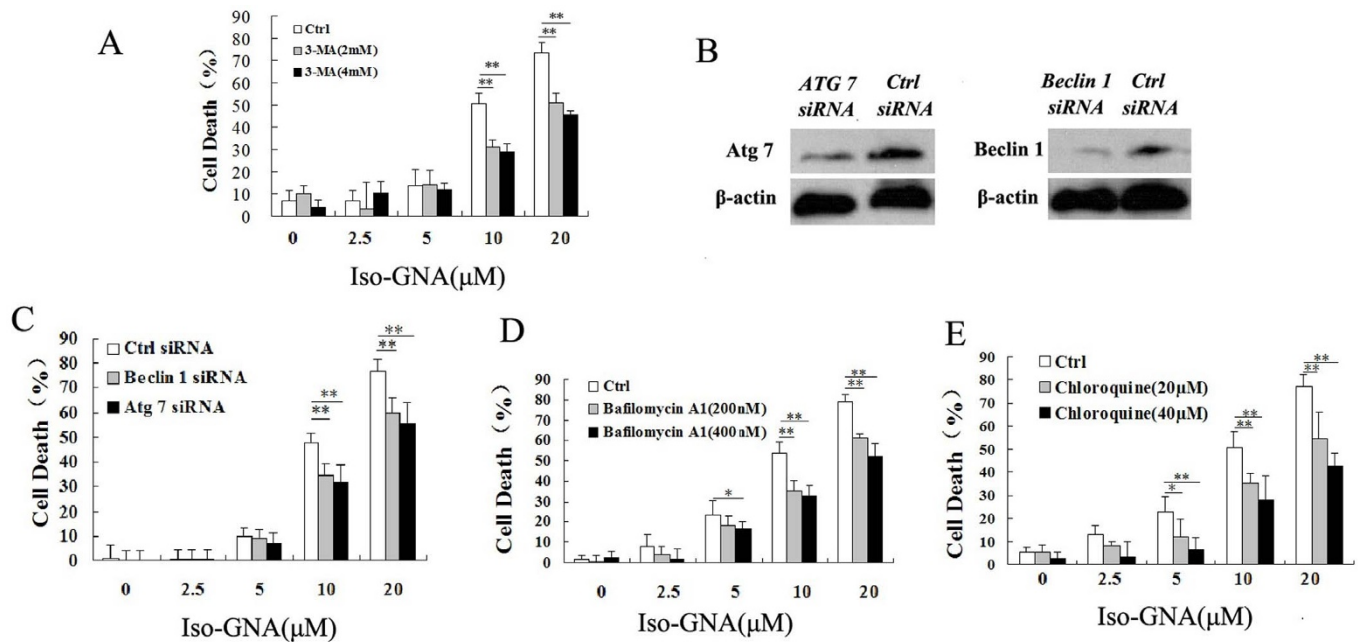


**Figure 4 | Iso-GNA Caused Cell Death in A549 Cells Was Autophagy-Dependent.** (A) Different concentrations iso-GNA with 0, 2 or 4 mM 3-MA were incubated with A549 cells for 24 h, then cells were stained with trypan blue to test death ratio. (B) Detection of Beclin1 or Atg7 expression by western blot in *Beclin1* or *Atg7* knock down A549 cells. (C) Different concentrations of iso-GNA were added to normal, *Beclin1* knock down or *Atg7* knock down A549 cells for 24 h, then trypan blue dye was employed to stain the cells and analyze the death ratio. (D) and (E) Different concentrations of iso-GNA with/without bafilomycin A1 (D) or chloroquine (E) were treated with A549 cells for 24 h, trypan blue dye was employed to stain the cells and analyze the death ratio. Data of three independent tests were shown as means  $\pm$  s.d. \* $p < 0.05$ ; \*\* $p < 0.01$ , in comparison with the untreated group. The whole images of western blots are given in Supplementary Figure S8.

proteins described above were up-regulated as a result of iso-GNA-induced autophagy. The data showed that the expression levels of Beclin1, Atg7 and the Atg5-Atg12 complex were significantly up-regulated in response to increasing concentrations of iso-GNA in both A549 and H460 cells (Fig. 3E and S2D).

#### Severe Autophagy Contributes to Iso-GNA-Induced Cell Death.

To investigate whether cancer cell death induced by iso-GNA in A549 cells was related to autophagy, both small molecular autophagy inhibitor (3-MA) and autophagy related gene (*Atg7* and *Beclin 1*) ablation were employed. We found that autophagy level and cell death caused by iso-GNA were obviously blocked by 3-MA dose-dependently in A549 cells (Fig.S3A and 4A). Then we used siRNA (*Atg7* and *Beclin 1*) knock down to inhibit autophagy. Western blot showed that siRNA could effectively inhibit the expression of *Atg7* and *Beclin1* (Fig. 4B). The results showed that both autophagy level and cell death ratio of knockdown cells were much lower in A549 cells treated with iso-GNA than control cells (Fig.S3D and 4C). The results described above effectively demonstrated that autophagy is the main contributor to cell death in iso-GNA treated A549 cells. To comprehensively validate autophagy is responsible for cell death caused by iso-GNA, we used bafilomycin A1, a lysosomal protease inhibitor, and chloroquine, an autophagolysosome fusion inhibitor. Both of these autophagy inhibitors inhibited the autophagy and cell death of A549 cells caused by iso-GNA (Fig. S3B, S3C, 4D and 4E). One thing needs to be noted here: bafilomycin A1, and chloroquine as inhibiting autophagosome degradation (late stage autophagy) which should usually result in an accumulation of autophagosomes. But we found that both of them could inhibit iso-GNA induced autophagosomes accumulation (Fig. S3B, S3C). So iso-GNA induced autophagosomes accumulation was kind of special and the mechanisms need to be further studied. All the above experiments were repeated in NSCLC H460 cells and similar

results were obtained (Fig. S4 and 5). These results demonstrated that cell death caused by iso-GNA was autophagy-dependent.

#### Iso-GNA-Induced Autophagic Cell Death With The Inhibition of Akt/mTOR Pathway.

Akt-mTOR pathway negatively regulates autophagy and is the main upstream pathway of autophagy<sup>29</sup>. Therefore we examined whether iso-GNA had effect on Akt-mTOR pathway intermediates by western blot. The results showed that the phosphorylation levels of both Akt and mTOR were remarkably reduced in iso-GNA-treated A549 and H460 cells (Fig. 6A and S5A). It is known that mTOR regulates protein synthesis by changing the phosphorylation level of both p70 S6K and 4E-BP1 during autophagy<sup>30</sup>. We therefore investigated the phosphorylation level of these two protein by western blot. We found the phosphorylation level of p70 S6K and 4E-BP1 were dose-dependently decreased by iso-GNA in both A549 and H460 cells (Fig. 6A and S5A). Rapamycin acts as an mTOR inhibitor and induces autophagy by forming a rapamycin-FKBP12 complex. The complex inhibits the activity of FRAP/mTOR<sup>31–32</sup>, and then inhibit p70 S6K and 4E-BP1<sup>33–34</sup>. Additionally, researchers have found that rapamycin is able to inhibit cell proliferation in malignant glioma cells<sup>35</sup>. This finding served as robust evidence for the important role of autophagic cell death in autophagy-inducer-controlled antineoplastic activity. Also, our study showed that co-treatment with iso-GNA and rapamycin led to stronger LC3 conversion and induction of cell death than iso-GNA or rapamycin treatment alone in A549 and H460 cells (Fig. 6B, 6C, S5B and S5C). Positive feedback from mTOR to Akt and Akt activation has been observed when rapamycin resistance occurs<sup>36–38</sup>. Previous studies showed that treatment with rapamycin and an Akt inhibitor to inhibit mTOR pathway could produce synergistic effects on autophagy<sup>39</sup>. Therefore, the synergistic effects on autophagy and Akt-mTOR pathway inhibition by the combination of iso-GNA and rapamycin could be a better approach for inducing autophagic cell death. Taken

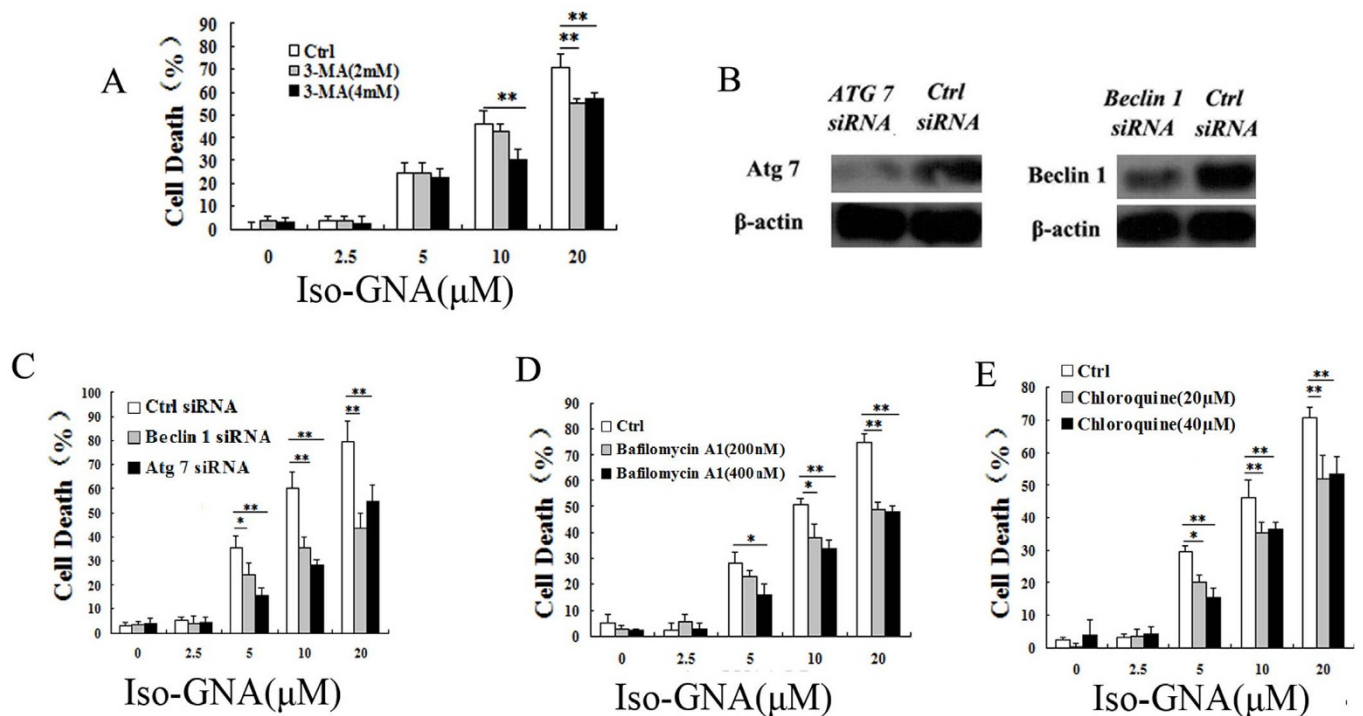


**Figure 5 | Iso-GNA causes autophagy-dependent cell death in H460 cells.** (A) Different concentrations of iso-GNA with 0, 2 or 4 mM 3-MA were added to H460 cells for 24 h, then cells were stained with trypan blue to test death ratio. (B) Detection of Beclin1 or Atg7 expression by western blot in *Beclin1* or *Atg7* knock down H460 cells. (C) Different concentrations of iso-GNA were added to normal, *Beclin1* knock down or *Atg7* knock down H460 cells for 24 h, then cells were stained with trypan blue to test death ratio. (D) and (E) Different concentrations of iso-GNA with/without bafilomycin A1 (D) or chloroquine (E) were treated with H460 cells for 24 h, trypan blue dye was employed to stain the cells and analyze the death ratio. Data of three independent tests were shown as means  $\pm$  s.d. \* $p < 0.5$ ; \*\* $p < 0.01$ , in comparison with the untreated group. The whole images of western blots are given in Supplementary Figure S9.

together, these findings suggested that Akt-mTOR-dependent signaling pathways is inhibited in iso-GNA-induced autophagy.

## Discussion

Here, we proposed that autophagy, but not apoptosis, most likely served as a main mechanism for iso-GNA-induced cell death. Several observations support our conclusions. First, no apoptosis was induced in iso-GNA-treated A549 and H460 cells (Fig. 2A, 2B and S1A). No obvious tunnel-positive cells or fields in iso-GNA-treated A549 were observed through tunnel assay in vivo (S1B). We further found that iso-GNA did not induce caspase 3 cleavage (Fig. 2C, S1C), which was in accordance with caspase 3 enzyme activity analysis (Fig. 2D, S1D). Most importantly, the cell death ratio caused by cisplatin rather than iso-GNA was evidently decreased by an apoptosis inhibitor, zVAD.fmk. This finding served as convincing evidence for non-apoptotic cell death in iso-GNA treated A549 and H460 cells (Fig. 2E and S1E). In addition, increased LC3 conversion, enhancement of p62 clearance and massive autophagic vacuolization (Fig. 3 and S2) in iso-GNA-treated cells suggested that autophagy was induced by iso-GNA. The second observation indicating that cell death induced by iso-GNA was autophagy-related was that cell death was obviously blocked by co-treatment of autophagy inhibitors or selectively ablation of *Atg7* or *Beclin1* through small interfering RNA (Fig. 4, 5). In accordance with our study, other reports have similarly indicated that autophagy may cause cancer cell death and autophagy inhibitors can reduce the death ratio. For example, autophagy inhibitor could reduce the death ratio in PC12D cells treated with caffeine<sup>40</sup>, human osteosarcoma cells treated with the plant alkaloid voacamine<sup>41</sup>, HeLa cells treated with the BCL2L1/BCL-XL inhibitor Z36<sup>42</sup>, HCT-116 treated with Bacillus Calmette-Guerin together with ionizing radiation<sup>43</sup> and human ovarian carcinoma cells treated with

monofunctional platinum (II) complex<sup>8</sup>. Finally, another observation indicating that cell death induced by iso-GNA was autophagy-related was the finding that the Akt-mTOR signaling pathway was inhibited in iso-GNA-treated A549 and H460 cells (Fig. 6A and S5A). In addition, iso-GNA-induced autophagic cell death was inhibited by the mTOR inhibitor rapamycin (Fig. 6C and S5C). Taken together, these data suggested the Akt-mTOR pathway was inhibited in iso-GNA-induced autophagy. The Akt-mTOR pathway is not only considered to be a negative regulator of autophagy but is also an inducer of G1 phase cell cycle arrest<sup>21,44</sup>. The G0/G1 phase cell cycle arrest observed in iso-GNA-treated A549 cells in this study (Fig. 2A) may also have resulted from the inhibition of the Akt-mTOR pathway by iso-GNA. Taken together, our data reveal that autophagy played an important role in cancer cell death caused by iso-GNA. Our study illustrated a clear mechanism of the antitumor activity of iso-GNA. This finding is of great importance for the development of effective methods to treat NSCLC patients whose tumors exhibit apoptosis defects.

Apart from apoptosis, which is a well studied cell death mechanism in cancer cells, autophagy also serves as a results to DNA damage<sup>45</sup>. Numerous apoptosis-targeting drugs have been developed<sup>46</sup>, such as cisplatin, which is a conventional platinum drug that induces apoptosis-dependent cell death in many human tumor cells<sup>47</sup>. However, researchers have still endeavored to examine how drugs target other cell death pathways because apoptosis resistance frequently developed in cancer cells, and it was found that targeting autophagic cell death may be an effective approach<sup>6,7,14,16</sup>. Reports showed that several chemotherapeutic agents including paclitaxel, doxorubicin and arsenic trioxide could induce non-apoptotic cancer cell death<sup>48,49</sup>. Thus, targeting autophagy could be an alternative approach for cancer treatment, especially for cancers with apoptosis



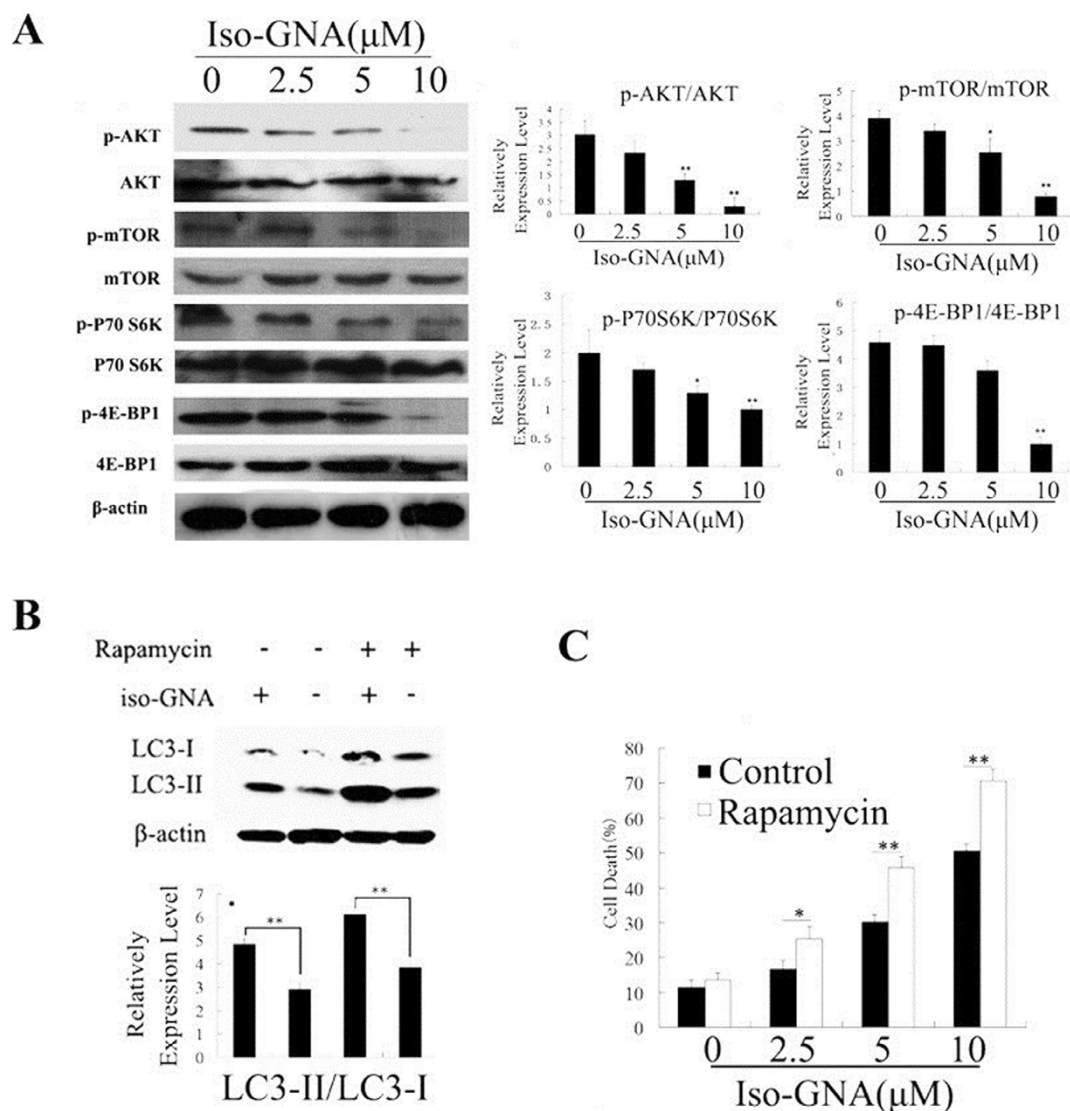


**Figure 6 | Iso-GNA induced autophagic cell death through the inhibition of Akt/mTOR Pathway.** (A) Western blot was used to detect the p-Akt, Akt, p-mTOR, mTOR, p-p70 S6K, p70 S6K, p-4E-BP1 and 4E-BP1 expression in various concentrations of iso-GNA treated A549 cells. (B) 0, 10  $\mu$ M of iso-GNA with or without 1  $\mu$ M rapamycin were added to A549 cells for 24 h, western blot was employed to detect the LC3 expression level. (C) The indicated concentration of iso-GNA with or without 1  $\mu$ M rapamycin were treated with A549 cells for 24 h, trypan blue dye was employed to stain the cells and analyze the death ratio. Data of three independent tests were shown as means  $\pm$  s.d. \*p < 0.05; \*\*p < 0.01, in comparison with the control group. The whole images of western blots are given in Supplementary Figure S10.

defects<sup>7,8,14,16</sup>. Additionally, some previous reports showed that cell death could be induced in an autophagy-dependent pathway when apoptosis is inhibited. For instance, the death of mouse L929 cells was controlled by *Atg7* and *Beclin1* when caspase was inhibited<sup>15</sup>. Etoposide-induced cell death in murine embryonic fibroblasts was inhibited by RNAi targeting *Atg5* and *Beclin1*<sup>50</sup>. Thus, it is important to note the effect of iso-GNA on autophagic cell death when the apoptosis machinery is absent in some cancers.

In summary, our current study revealed that iso-GNA induces apoptosis-independent autophagic cell death in human NSCLC cells and inhibits the Akt-mTOR pathway. Iso-GNA may be an effective chemotherapeutic agent against NSCLC in a clinical setting.

## Methods

**Reagents, cell lines and cell culture.** Iso-GNA was obtained as described in our previous study<sup>23</sup> to a purity of greater than 98%. For all *in vitro* assays, Iso-GNA (20mM) was dissolved in DMSO (dimethyl sulphoxide), preserved at room temperature and then diluted to required concentration when needed. For all animal studies, Iso-GNA was dissolved in sodium chloride injection (154 mmol/L, pH = 6.5)

containing 3% sterile ethanol (100% sterile ethanol, then diluted to 3% ethanol with sodium chloride). DMSO, MTT, cisplatin, bafilomycin A1, chloroquine, zVAD.fmk, 3-MA, DAPI and rapamycin were obtained from Sigma Aldrich. Antibodies were obtained from the following sources: Atg5 (Abcam), Atg7 (Abcam), Akt (Cell Signaling Technology), Beclin 1 (Santa Cruz),  $\beta$ -actin (Santa Cruz), SQSTM1/p62 (Sigma), LC3 (Abcam), phospho-Akt (Cell Signaling Technology), mTOR (Millipore), phospho-mTOR (Millipore), caspase 3 (Millipore), p70 S6K (Santa Cruz), phospho-p70 S6K (Santa Cruz), 4E-BP1 (Santa Cruz), phospho-4E-BP1 (Santa Cruz), HRP-labeled anti-rabbit and mouse secondary antibody (Santa Cruz), *Atg7* siRNA I and *Beclin1* siRNA I (Cell Signaling Technology). A549 and H460 cell lines were obtained from ATCC (the American Type Culture Collection). HepG2, HeLa, and HCT-116 cell lines were obtained from the Shanghai Institute of Cell Biology. Cells were cultured in a humidified atmosphere containing 5% CO<sub>2</sub> (37°C). The culture medium RPMI 1640 (Containing 10% fetal bovine serum, 100  $\mu$ g/ml streptomycin and 100 U/ml penicillin) was obtained from ATCC.

**Cell viability assays.** (1) MTT Assay: Described in our previous study<sup>23</sup> (2) Trypan Blue Exclusion Assay. 6-well culture plates were used for cell culture. After incubated for 24 hours, various concentrations of iso-GNA were added to cells for another 24 hours. Both alive and dead cells were collected after wash with PBS, and then stained with trypan blue dye (0.4 mg/ml in PBS) for 6 min. Then cells were counted with a hemocytometer to calculate the death ratio.



**Cell cycle analysis.** 6-well culture plates were used for cell culture. After incubated for 24 hours, various concentrations of iso-GNA were added to cells for another 24 hours. The alive cells were collected and washed with PBS for two times, then fixed with 75% (v/v) pre-cold ethanol at 4°C for 12 hours. Cells were washed with PBS for three times and then stained with PI staining buffer (PI, 50 µg/ml) for 20 min. The cell cycle were then subjected to flow cytometry to analyze cell cycle. Approximately 30,000 cells were evaluated for each sample.

**Annexin V-FITC/PI Apoptosis Assay.** 6-well culture plates were used for cell culture. After incubated for 24 hours, various concentrations of iso-GNA were added to cells for another 24 hours. Then cells were collected and digested into single cell suspensions with EDTA-free trypsin and then subjected to the Annexin V/PI Apoptosis Detection kit (Invitrogen) for staining according to the manufacturer's instructions. The stained cells were analyzed by flow cytometry in one hour after staining.

**Western blot.** Both alive and dead cells were collected and washed with pre-cold PBS. The total cell protein lysates was obtained using RIPA Lysis Buffer. After denaturalization, about 25 µg lysates were loaded on SDS-PAGE. After electrophoresis on SDS-PAGE, the gels were transferred to PVDF (polyvinylidene difluoride) membranes electrophoretically at 4°C for 2.5 hours. Then 5% skim milk in 1 × PBST was employed to blocked the PVDF membranes. The first antibodies were then diluted in blocking buffer and incubated with membranes at 4°C for 12 hours. Then, the membranes were washed with 1 × PBST (3 × 15 min) and then incubated with secondary antibodies for 2 hour. Immunoreactivity detection was accomplished by using enhanced chemiluminescence reagents (Millipore).

**TUNEL Assay.** To examine the apoptosis cells in tumor section, we used the In Situ Cell Death Detection Kit (Roche Applied Science) by following the manufacturer's instructions, then the tissue section was detected and imaged under a fluorescence microscope.

**Transfection and LC3-RFP counting.** The plasmid was transfected to A549 cells using Lipofectamine 2000 (Invitrogen) according to instructions of the manufacturer. G418 (Sigma-Aldrich) was used to select stable transformants. Cells stably expression LC3-RFP were cultured in EBSS (Sigma-Aldrich) culture to induce autophagy (Figure. S2C). A549 cells stably expressing RFP-LC3 were treated with iso-GNA for 24 hours and then subjected to a Leica aser-scanning spectrum confocal system to count RFP dots. RFP-LC3 positive cells were these cells which contained 10 or more RFP punctate dots.

**Autophagy detection by GFP-LC3 expression.** The plasmid was transfected to A549 or H460 cells using Lipofectamine 2000 (Invitrogen) according to instructions of the manufacturer. At 24 h after transfection, iso-GNA with or without autophagy inhibitors was added to the cells. After incubation for 12 hours, the GFP-LC3 positive cells were detected and imaged under a fluorescence microscope.

**Transmission electron microscopy and Immunohistochemistry.** Described in previous study<sup>51</sup>.

**Tumor xenograft model.** Tumors were initiated by subcutaneous injection of tumour cell suspension (A549, 18000 cells per mouse) into the front of right backside of mice. When A549 tumour xenografts reached about 70 mm<sup>3</sup> in size, the mice were divided into three groups of six each randomly. The test group received intravenous (i.v.) injections of iso-GNA (20 mg/kg in a volume of 200 µl) via tail vein every two days. The control group received intravenous (i.v.) injections of an equal volume of vehicle. The positive group were treated with cisplatin (4 mg/kg, IP) two times per week. The tumour volume were recorded every 3 days and were calculated with the formulas: tumour volume (mm<sup>3</sup>) = (length × width<sup>2</sup>) × 0.52. Animals were sacrificed 24 d after injection.

**Statistical analysis.** Statistics results of multiple experiments were shown expressed as means ± s.d. Student's t-test and one-way ANOVA test were employed for data analysis. Significance was determined with P values of ≤0.05.

**Ethics statement.** All the methods were carried out in accordance with the approved guidelines and the entire experimental procedures were carried out under the guidance of Institutional Animal Care and Use Committee of Sichuan University (Chengdu, China).

1. Ferlay, J. *et al.* Estimates of worldwide burden of cancer in 2008: GLOBOCAN 2008 [J]. *Int. J. Cancer* **127**, 2893–2917 (2010).
2. Ferreira, C. G., Tolis, C. & Giaccone, G. p53 and chemosensitivity [J]. *Ann. Oncol.* **10**, 1011–1021 (1999).
3. El-Deiry, W. S. The role of p53 in chemosensitivity and radiosensitivity [J]. *Oncogene* **22**, 7486–7495 (2003).
4. White, E. Autophagic cell death unraveled: Pharmacological inhibition of apoptosis and autophagy enables necrosis. *Autophagy* **4**, 399–401 (2008).
5. Shen, H. M. & Codogno, P. Autophagic cell death: Loch Ness monster or endangered species? *Autophagy* **7**, 457–465 (2011).

6. Kondo, Y. & Kondo, S. Autophagy and cancer therapy. *Autophagy* **2**, 85–90 (2006).
7. Levy, J. M. & Thorburn, A. Targeting autophagy during cancer therapy to improve clinical outcomes. *Pharmacol. Ther.* **131**, 130–141 (2011).
8. Guo, W. J. *et al.* Novel monofunctional platinum (II) complex induces apoptosis-independent autophagic cell death in human ovarian carcinoma cells, distinct from cisplatin [J]. *Autophagy* **9**, 996–1008 (2013).
9. O'Donovan, T. R., O'Sullivan, G. C. & McKenna, S. L. Induction of autophagy by drug-resistant esophageal cancer cells promotes their survival and recovery following treatment with chemotherapeutics. *Autophagy* **7**, 509–524 (2011).
10. Li, J., Hou, N., Faried, A., Tsutsumi, S. & Kuwano, H. Inhibition of autophagy augments 5-fluorouracil chemotherapy in human colon cancer in vitro and in vivo model. *Eur. J. Cancer* **46**, 1900–1909 (2010).
11. Zhu, K., Dunner, K. J. & McConkey, D. J. Proteasome inhibitors activate autophagy as a cytoprotective response in human prostate cancer cells. *Oncogene* **29**, 451–462 (2010).
12. Vazquez-Martin, A., Oliveras-Ferraro, C. & Menendez, J. A. Autophagy facilitates the development of breast cancer resistance to the anti-HER2 monoclonal antibody trastuzumab. *PLoS One* **4**, e6251 (2009).
13. Wu, Z. *et al.* Autophagy blockade sensitizes prostate cancer cells towards Src family kinase inhibitors. *Genes Cancer* **1**, 40–49 (2010).
14. Mujumdar, N. & Saluja, A. K. Autophagy in pancreatic cancer: an emerging mechanism of cell death. *Autophagy* **6**, 997–998 (2010).
15. Yu, L. *et al.* Regulation of an Atg7-beclin 1 program of autophagic cell death by caspase-8. *Science* **304**, 1500–1502 (2004).
16. Amaravadi, R. K. *et al.* Principles and current strategies for targeting autophagy for cancer treatment. *Clin. Cancer Res.* **17**, 654–656 (2011).
17. Liu, E. Y. & Ryan, K. M. Autophagy and cancer—issues we need to digest. *J. Cell Sci.* **125**, 2349–2358 (2012).
18. Xie, Z. & Klionsky, D. J. Autophagosome formation: core machinery and adaptations. *Nat. Cell Biol.* **9**, 1102–1109 (2007).
19. Geng, J. & Klionsky, D. J. The Atg8 and Atg12 ubiquitinlike conjugation systems in macroautophagy. 'Protein modifications: beyond the usual suspects' review series. *EMBO Rep.* **9**, 859–864 (2008).
20. Kroemer, G., Mariño, G. & Levine, B. Autophagy and the integrated stress response. *Mol. Cell* **40**, 280–293 (2010).
21. Yang, Z. & Klionsky, D. J. Mammalian autophagy: core molecular machinery and signaling regulation. *Curr. Opin. Cell Biol.* **22**, 124–131 (2010).
22. Pandey, M. K. *et al.* Gambogic acid, a novel ligand for transferrin receptor, potentiates TNF-induced apoptosis through modulation of the nuclear factor-κB signaling pathway [J]. *Blood* **110**, 3517–3525 (2007).
23. Fan, Y. *et al.* Isogambogic acid inhibits tumour angiogenesis by suppressing Rho GTPases and vascular endothelial growth factor receptor 2 signalling pathway. *J. Chemother.* **25**, 298–308 (2013).
24. Klionsky, D. J., Cuervo, A. M. & Seglen, P. O. Methods for monitoring autophagy from yeast to human. *Autophagy* **3**, 181–206 (2007).
25. Moscat, J. & Diaz-Meco, M. T. p62 at the crossroads of autophagy, apoptosis, and cancer. *Cell* **137**, 1001–1004 (2009).
26. Kroemer, G. *et al.* Nomenclature Committee on Cell Death 2009. Classification of cell death: recommendations of the Nomenclature Committee on Cell Death 2009. *Cell Death Differ.* **16**, 3–11 (2009).
27. Yang, Z. & Klionsky, D. J. An overview of the molecular mechanism of autophagy. *Curr. Top Microbiol. Immunol.* **335**, 1–32 (2009).
28. Luo, S. & Rubinsztein, D. C. Atg5 and Bcl-2 provide novel insights into the interplay between apoptosis and autophagy. *Cell Death Differ.* **14**, 1247–1250 (2007).
29. Hanahan, D. & Weinberg, R. A. Hallmarks of cancer: the next generation. *Cell* **144**, 646–674 (2011).
30. Pouyssegur, J., Dayan, F. & Mazure, N. M. Hypoxia signaling in cancer and approaches to enforce tumour regression. *Nature* **441**, 437–443 (2006).
31. Brown, E. J. *et al.* A mammalian protein targeted by G1-arresting rapamycin-receptor complex. *Nature* **369**, 756–758 (1994).
32. Kunz, J. *et al.* Target of rapamycin in yeast, TOR2, is an essential phosphatidylinositol kinase homolog required for G1 progression. *Cell* **73**, 585–596 (1993).
33. Jefferies, H. B. *et al.* Rapamycin suppresses 5' TOP mRNA translation through inhibition of p70s6k. *EMBO J.* **16**, 3693–3704 (1997).
34. Beretta, L. *et al.* Rapamycin blocks the phosphorylation of 4E-BP1 and inhibits cap-dependent initiation of translation. *EMBO J.* **15**, 658–664 (1996).
35. Takeuchi, H. *et al.* Synergistic augmentation of rapamycin-induced autophagy in malignant glioma cells by phosphatidylinositol 3-kinase/protein kinase B inhibitors. *Cancer Res.* **65**, 3336–3346 (2005).
36. Shi, Y., Yan, H., Frost, P., Gera, J. & Lichtenstein, A. Mammalian target of rapamycin inhibitors activate the AKT kinase in multiple myeloma cells by up-regulating the insulin-like growth factor receptor/insulin receptor substrate-1/ phosphatidylinositol 3-kinase cascade. *Mol. Cancer Ther.* **4**, 1533–1540 (2005).
37. O'Reilly, K. E. *et al.* mTOR inhibition induces upstream receptor tyrosine kinase signaling and activates Akt. *Cancer Res.* **66**, 1500–1508 (2006).
38. Wan, X. *et al.* Rapamycin induces feedback activation of Akt signaling through an IGF-1R-dependent mechanism. *Oncogene* **26**, 1932–1940 (2007).





39. Cirstea, D. *et al.* Dual inhibition of akt/mammalian target of rapamycin pathway by nanoparticle albumin-bound rapamycin and perifosine induces antitumor activity in multiple myeloma. *Mol. Cancer Ther.* **9**, 963–975 (2010).
40. Saiki, S. *et al.* Caffeine induces apoptosis by enhancement of autophagy via PI3K/Akt/mTOR/p70S6K inhibition. *Autophagy* **7**, 176–187 (2011).
41. Meschini, S. *et al.* The plant alkaloid voacamine induces apoptosis-independent autophagic cell death on both sensitive and multidrug resistant human osteosarcoma cells. *Autophagy* **4**, 1020–1033 (2008).
42. Lin, J. *et al.* A novel Bcl-XL inhibitor Z36 that induces autophagic cell death in HeLa cells. *Autophagy* **5**, 314–520 (2009).
43. Yuk, J. M. *et al.* Bacillus calmette-guerin cell wall cytoskeleton enhances colon cancer radiosensitivity through autophagy. *Autophagy* **6**, 46–60 (2010).
44. Barbet, N. C. TOR controls translation initiation and early G1 progression in yeast. *Mol. Biol. Cell* **7**, 25–42 (1996).
45. Matsui, A., Kamada, Y. & Matsuura, A. The Role of Autophagy in Genome Stability through Suppression of Abnormal Mitosis under Starvation [J]. *PLoS genetics* **9**, e1003245 (2013).
46. Sun, S. Y., Hail, N. J. & Lotan, R. Apoptosis as a novel target for cancer chemoprevention. *J. Natl. Cancer Inst.* **96**, 662–672 (2004).
47. Vakifahmetoglu, H. *et al.* DNA damage induces two distinct modes of cell death in ovarian carcinomas. *Cell Death Differ.* **15**, 555–566 (2008).
48. Bröker, L. E., Kruyt, F. & Giaccone, G. Cell death independent of caspases: a review. *Clin. Cancer Res.* **11**, 3155–3162 (2005).
49. Chen, T. S. *et al.* Taxol induces caspase-independent cytoplasmic vacuolization and cell death through endoplasmic reticulum (ER) swelling in ASTC-a-1 cells. *Cancer Lett.* **270**, 164–172 (2008).
50. Shimizu, S. *et al.* Role of Bcl-2 family proteins in a non-apoptotic programmed cell death dependent on autophagy genes. *Nat. Cell Biol.* **6**, 1221–1228 (2004).
51. Wang, K. *et al.* Quercetin induces protective autophagy in gastric cancer cells: involvement of Akt-mTOR-and hypoxia-induced factor 1 $\alpha$ -mediated signaling. *Autophagy*, **7**, 966–978 (2011).

## Acknowledgments

We thank Professor Canhua Huang (State Key Laboratory of Biotherapy; West China Hospital; West China Medical School; Sichuan University; Chengdu, China) for providing the Beclin1, Atg7 and Atg5 antibodies. This work was supported by grants from the National High Tech R&D Program of China (2014AA022202) and the Natural Science Foundation of China (81373283).

## Author contributions

J.-H.Y., Y.-Z.Z. and X.C. carried out most of the cellular, biochemical experiments. Y.F. performed the animal experiments. H.-S.C., S.-C.L. and H.-Y.Y. performed the separation of isogambogenic acid and identified the structure of iso-GNA. C.-F.X., W.-W.S., C.-Y.L., H.-Y.P., L.-Y.L. and Z.W. performed a part of cellular experiments. A.-H.P. analyzed most of the data. Y.-Q.W., W.-M.L. and L.-J.C. designed the project and led the team to accomplish it. All authors reviewed the manuscript.

## Additional information

**Supplementary information** accompanies this paper at <http://www.nature.com/scientificreports>

**Competing financial interests:** The authors declare no competing financial interests.

**How to cite this article:** Yang, J. *et al.* Isogambogenic acid induces apoptosis-independent autophagic cell death in human non-small-cell lung carcinoma cells. *Sci. Rep.* **5**, 7697; DOI:10.1038/srep07697 (2015).



This work is licensed under a Creative Commons Attribution-NonCommercial-ShareAlike 4.0 International License. The images or other third party material in this article are included in the article's Creative Commons license, unless indicated otherwise in the credit line; if the material is not included under the Creative Commons license, users will need to obtain permission from the license holder in order to reproduce the material. To view a copy of this license, visit <http://creativecommons.org/licenses/by-nc-sa/4.0/>